

# Scanning Electrochemical Microscopy: Using the Potentiometric Mode of SECM To Study the Mixed Potential Arising from Two Independent Redox Processes

Mara Serrapede,<sup>†</sup> Guy Denuault,<sup>\*,†</sup> Maciej Sosna,<sup>‡</sup> Giovanni Luca Pesce,<sup>§</sup> and Richard J. Ball<sup>§</sup>

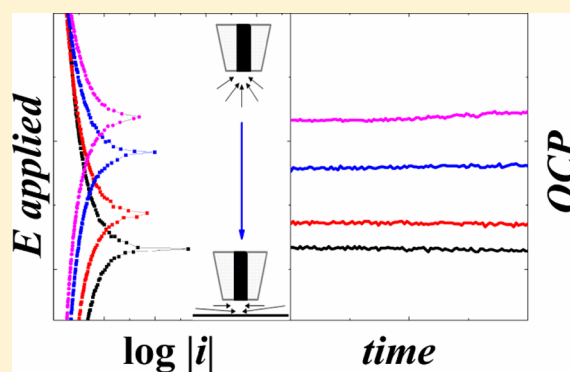
<sup>†</sup>School of Chemistry, University of Southampton, SO17 1BJ, Southampton, U.K.

<sup>‡</sup>Interdisciplinary Nanoscience Center (iNANO), Aarhus University, Gustav Wieds vej 14, DK-8000, Aarhus C, Denmark

<sup>§</sup>Department of Architecture & Civil Engineering, University of Bath, BA2 7AY, Bath, U.K.

## S Supporting Information

**ABSTRACT:** This study demonstrates how the potentiometric mode of the scanning electrochemical microscope (SECM) can be used to sensitively probe and alter the mixed potential due to two independent redox processes provided that the transport of one of the species involved is controlled by diffusion. This is illustrated with the discharge of hydrogen from nanostructured Pd hydride films deposited on the SECM tip. In deaerated buffered solutions the open circuit potential of the PdH in equilibrium between its  $\beta$  and  $\alpha$  phases ( $OCP_{\beta \rightarrow \alpha}$ ) does not depend on the tip–substrate distance while in aerated conditions it is found to be controlled by hindered diffusion of oxygen. Chronopotentiometric and amperometric measurements at several tip–substrate distances reveal how the flux of oxygen toward the Pd hydride film determines its potential. Linear sweep voltammetry shows that the polarization resistance increases when the tip approaches an inert substrate. The SECM methodology also demonstrates how dissolved oxygen affects the rate of hydrogen extraction from the Pd lattice. Over a wide potential window, the highly reactive nanostructure promotes the reduction of oxygen which rapidly discharges hydrogen from the PdH. The flux of oxygen toward the tip can be adjusted via hindered diffusion. Approaching the substrate decreases the flux of oxygen, lengthens the hydrogen discharge, and shifts  $OCP_{\beta \rightarrow \alpha}$  negatively. The results are consistent with a mixed potential due to the rate of oxygen reduction balancing that of the hydride oxidation. The methodology is generic and applicable to other mixed potential processes in corrosion or catalysis.



In the potentiometric mode of SECM the tip is generally considered to behave as a passive probe whose potential reflects the activity of the species of interest. It is therefore unable to consume or produce species, and thus its applications are limited compared to its amperometric counterpart. The potentiometric mode nevertheless possesses advantages, notably, the numerous ion-selective electrodes available enable detection, with high sensitivity and selectivity, of a range of species not redox active in aqueous media; see ref 1 for an in-depth review of this mode. The potentiometric response is known to be affected by Ohmic drops when current flows within the cell,<sup>2</sup> and this must be taken into account when varying the tip–substrate distance. However, to our knowledge, there is no report of the potentiometric response of an SECM tip being affected by Faradaic processes on the tip. The aim of this article is therefore to demonstrate that the tip can produce a mixed potential dependent on the diffusion of one species and follow a tip–substrate distance dependence analogous to an amperometric feedback response. To illustrate this effect, we use the potentiometric response of a nanostructured Pd tip

loaded with hydrogen so that its potential is only determined by the solution pH.

Palladium is well-known for its ability to absorb hydrogen<sup>3,4</sup> and for the possibility to measure pH potentiometrically when the hydrogen to Pd ratio (H/Pd) is between 0.02 and 0.6, i.e. when the hydride is in the transition between its  $\alpha$  and  $\beta$  phases.<sup>5</sup> Exploiting this property Imokawa et al.<sup>6</sup> fabricated reliable micrometer pH sensors by loading hydrogen into nanostructured Pd films electrodeposited on Pt microdisc electrodes. The nanostructure was obtained by electrodepositing Pd within the hexagonal phase of a lyotropic liquid crystal according to the procedure previously reported.<sup>7,8</sup> In absence of oxygen, the nanostructured palladium hydride tips are sensitive only to the activity of the protons and they have a virtually Nernstian response with a slope ca.  $-58.7$  mV/pH at 25 °C from pH 2 to 14.<sup>6,9</sup> However dissolved oxygen seriously affects their potentiometric response.<sup>6</sup> In the bulk, the lifetime of a 25

Received: June 7, 2013

Accepted: August 6, 2013

Published: August 6, 2013

$\mu\text{m}$   $\varnothing$  PdH sensor is ca. 60 times shorter when the solution is saturated with oxygen than with argon.<sup>9</sup> Moreover, the open circuit potential recorded during the discharge of the hydride is more positive in an oxygenated solution. Using the SECM with a combination of potentiometric and amperometric techniques, we assess the rate of H extraction in an aerated buffered solution and investigate the dependence of the PdH open circuit potential on the flux of oxygen. Experimental data are analyzed in terms of a simple mixed potential model.

## EXPERIMENTAL SECTION

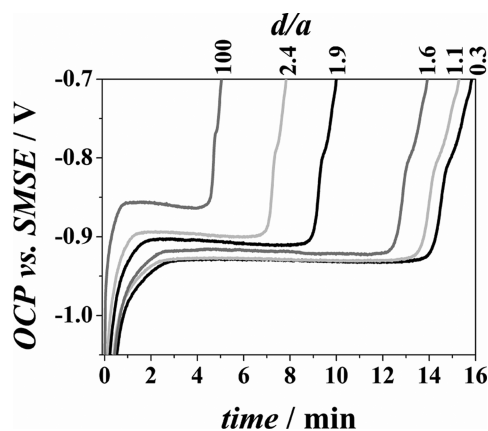
All experiments were carried out in a grounded aluminum Faraday cage, at room temperature ( $20 \pm 2$  °C) with solutions equilibrated in air for at least 48 h, unless otherwise stated. All the glassware was soaked overnight in 5% Decon 90 (BDH) and rinsed thoroughly with pure water before use. SECM tips were made as reported previously<sup>6</sup> by sealing a Pt microwire (typically 25  $\mu\text{m}$   $\varnothing$  from Goodfellow metals Ltd.) in borosilicate glass pipettes. The front of the tip was ground using silicon carbide papers (from 320 to 1200 grit) and then with alumina powder (1 then 0.3  $\mu\text{m}$   $\varnothing$ ) supported on polishing cloth (Buehler) to a mirror finish, washed, and sonicated in purified water. The sides of the microdisc were ground to form a truncated cone with a radius of glass,  $r_g$ , sufficiently small to enable close approach of the substrate. All reagents were used without further purification. The nanostructured Pd film was prepared by potentiostatically (0.1 V vs SCE) electrodepositing Pd onto the Pt microdisc from a mixture consisting of 47 wt % Brij 56 ( $\text{C}_{16}\text{EO}_m$ ,  $n = 4-12$ ) from Aldrich, 12 wt %  $(\text{NH}_4)_2\text{PdCl}_4$  from Alfa Aesar, 2 wt % heptane from BDH, and 39 wt % water from a Purite Select water purification system. A charge of ca. 4  $\mu\text{C}$  was passed to produce a film roughly 1.8  $\mu\text{m}$  thick; see SEM image in Figure SI-1, Supporting Information. The radius of the Pd deposit,  $a$ , and the RG ( $r_g/a$ ) were measured by SEM (using a gaseous secondary electron detector, 0.6 Torr water vapor, and 10 kV) with an XL30 ESEM environmental scanning electron microscope (FEI). All electrochemical experiments were conducted in a three-electrode configuration with an Autolab PGSTAT 101 (Ecochemie) programmed with Nova 1.9. The SECM tip was positioned with PI M-605 high-accuracy translation stages controlled by PIMikroMove software (all from Physik Instruments GmbH & Co.). All approach curves were recorded from the bulk to the substrate at 1  $\mu\text{m s}^{-1}$ . The SECM cell was homemade from Perspex with microscope slides glued on both sides to facilitate viewing of the probe. The substrate was either a glass slide or the bottom of the cell. The counter electrode was a platinum mesh located in a side compartment; the reference electrode was a homemade Hg/Hg<sub>2</sub>SO<sub>4</sub>-saturated K<sub>2</sub>SO<sub>4</sub> electrode (SMSE) connected to the cell via a capillary salt bridge (1 wt % Agar in saturated K<sub>2</sub>SO<sub>4</sub>). The capillary was attached to the tip to ensure that the distance between the capillary opening and tip remained constant whatever the tip–substrate distance. The nanostructured Pd tips were checked by voltammetry in 1 M H<sub>2</sub>SO<sub>4</sub>, sweeping between the start of hydrogen evolution and the foot of oxygen evolution until the characteristic voltammetric features of Pd in acid were obtained; see Figure SI-2 (Supporting Information) for a typical voltammogram. Their diffusional properties were assessed by recording linear sweep voltammograms in 5 mM Ru(NH<sub>3</sub>)<sub>6</sub>Cl<sub>3</sub> in 0.5 M KCl. They were subsequently loaded with hydrogen galvanostatically (stepping from 0 to –80 nA for typically 100 s) to reach a H/Pd ratio of 0.6 corresponding to

the  $\beta$  phase of the hydride. Figure SI-3 (Supporting Information) shows a typical chronopotentiogram recorded during the galvanostatic loading of H. All SECM experiments were carried out in a 200 mM ionic strength,  $I_s$ , pH 7 or 7.5 solution prepared from 20 mM NaH<sub>2</sub>PO<sub>4</sub> (Analar grade, Aldrich), Na<sub>2</sub>SO<sub>4</sub> (Analar grade, Sigma). Solutions were deaerated by purging with Ar (99.99%, BOC). Potentiometric approach curves were recorded with  $0.6 < \text{H/Pd} < 0.02$  to ensure that the hydride composition did not influence the tip potential.

## RESULTS AND DISCUSSION

### Potentiometric and Amperometric Observations.

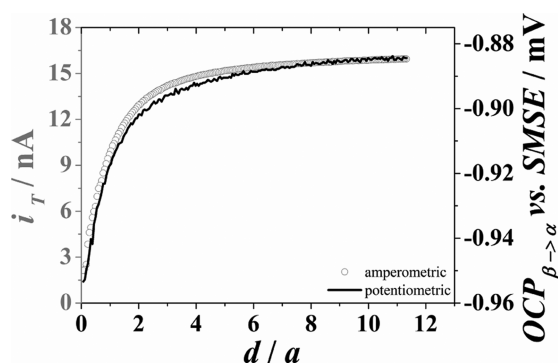
Figure 1 shows a set of chronopotentiograms recorded at



**Figure 1.** Chronopotentiograms recorded at several tip–substrate distances,  $d$ , in an aerated pH 7 buffer solution ( $I_s = 200$  mM).  $a = 18.7$   $\mu\text{m}$ , RG = 6.

different tip–substrate distances above the inert substrate in the aerated phosphate buffer. They all show features characteristic of the loss of hydrogen from the Pd lattice. At sort times, the potential rises sharply as the  $\beta$  phase loses hydrogen and then reaches a plateau ( $\text{OCP}_{\beta \rightarrow \alpha}$ ) when the  $\alpha$  phase begins to nucleate within the  $\beta$  phase. This is the transition region where the phase rule dictates that the electrode potential only depends on the activity of the protons in solution but not on the H/Pd. Only in this region can the electrode be used as a pH sensor. At the end of the plateau, the potential rises as the entire PdH is now in the  $\alpha$  phase. At longer times, a further shoulder is observed which is thought to reflect H desorption from the Pd surface. All these observations are consistent with previous observations at nanostructured Pd microdiscs.<sup>6</sup> Surprisingly, all the chronopotentiograms depend on the tip–substrate distance. As the tip approaches the inert substrate, the most striking observation is the significant increase in the lifetime of the phase transition plateau. The second important observation is that the plateau potential,  $\text{OCP}_{\beta \rightarrow \alpha}$ , becomes more negative as the tip approaches the substrate. This cannot be due to a change of pH as the solution is buffered nor can it be due to the tip sensing an Ohmic drop, as there is no current flowing within the cell. Such a potential shift would be a major problem if the tip were to be used to monitor pH.

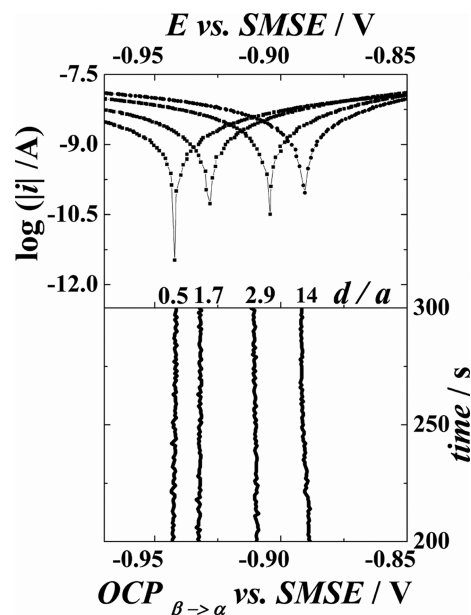
A potentiometric approach curve recorded to assess the dependence of  $\text{OCP}_{\beta \rightarrow \alpha}$  on the tip–substrate distance is shown in Figure 2. The duration of the approach curve was kept shorter than the duration of the  $\beta$  to  $\alpha$  transition to prevent any variation of the tip potential with the hydride composition.



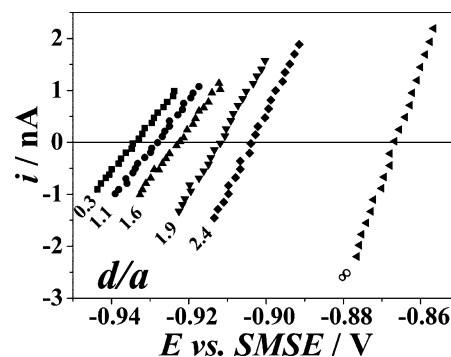
**Figure 2.** Comparison between potentiometric (right Y-axis) and amperometric (left Y-axis) approach curves recorded with a nanostructured Pd tip at  $1 \mu\text{m s}^{-1}$  in an aerated pH 7 phosphate buffer solution ( $I_s = 200 \text{ mM}$ );  $\text{RG} = 3.3$ ,  $a = 18.7 \mu\text{m}$ . The amperometric response was taken at  $-0.6 \text{ V}$  vs SMSE to ensure that the ORR was diffusion controlled. The potentiometric response is the open circuit potential taken in the  $\beta$  to  $\alpha$  transition region of the palladium hydride.

Figure 2 confirms that the potential becomes more negative as the tip–substrate distance decreases. Surprisingly, the dependence of the potential on the tip–substrate distance matches the amperometric approach curve recorded with the same tip for the reduction of dissolved oxygen. The latter is in perfect agreement with the theoretical curve for hindered diffusion,<sup>10</sup> Figure SI-4 (Supporting Information), thereby confirming that the nanostructured film is sufficiently thin to behave as a disc. Figure 2 clearly suggests that the potentiometric response is driven by a process analogous to hindered diffusion at all tip–substrate distances. The only redox active species present in solution being oxygen, the tip potential must be related to the rate of the oxygen reduction reaction (ORR). Palladium is known as a good catalyst for promoting the ORR,<sup>11,12</sup> and the nanostructured palladium is expected to be even better as found for nanostructured Pt tips prepared by the same method.<sup>13</sup> As a result, the wave for ORR occurs at very positive potentials (ca.  $-0.1 \text{ V}$  vs SMSE), Figure SI-5 (Supporting Information), and  $\text{OCP}_{\beta \rightarrow \alpha}$  is more negative than the potential for the ORR wave. The potential difference is sufficiently large that the nanostructured PdH tip promotes the ORR at a diffusion-controlled rate at all pH. In the presence of oxygen, two Faradaic processes are therefore balanced at  $\text{OCP}_{\beta \rightarrow \alpha}$ : the electrochemical oxidation of the hydride and the electrochemical reduction of the oxygen. Any increase in oxygen flux toward the tip is matched by an increase in the PdH oxidation rate and therefore by a larger hydrogen extraction rate. In the next section we investigate how the latter depends on the tip–substrate distance through a series of Tafel, Figure 3, and linear polarization resistance (LPR) measurements, Figure 4.

**Hydrogen Extraction Rate Dependence on Tip–Substrate Distance.** Linear sweep voltammograms were recorded at  $1 \text{ mV s}^{-1} \pm 100 \text{ mV}$  around  $\text{OCP}_{\beta \rightarrow \alpha}$  for different oxygen fluxes obtained by varying the tip–substrate distance. These results are presented as Tafel plots in the top part of Figure 3. The equilibrium potentials found with the potential sweeps are in agreement with the  $\text{OCP}_{\beta \rightarrow \alpha}$  values measured by chronopotentiometry at the same tip positions, bottom part of Figure 3. The corresponding exchange currents, from now on called hydrogen extraction currents, were estimated from the intercept between the cathodic Tafel branch and the vertical line corresponding to the equilibrium potential. Finding a clear linear region over one decade of current proved difficult; for



**Figure 3.** Comparison between Tafel experiments (top) and chronopotentiograms at  $\text{OCP}_{\beta \rightarrow \alpha}$  (bottom) recorded at the tip–substrate distances indicated by  $d/a$ . Linear sweep voltammograms were taken at  $1 \text{ mV s}^{-1}$  around  $\text{OCP}_{\beta \rightarrow \alpha}$ .



**Figure 4.** Linear sweep voltammograms recorded at  $1 \text{ mV s}^{-1}$  around  $\text{OCP}_{\beta \rightarrow \alpha}$  to determine the linear polarization resistance at the tip–substrate distances indicated by  $d/a$ .

this reason, the extraction currents,  $i_{T,\text{ex}}$ , were also estimated from the polarization resistance ( $i_{T,\text{ex}} = RT/nFR_p$ ) determined from the gradient of linear sweep voltammograms taken within  $10 \text{ mV}$  of the equilibrium potential for several tip–substrate distances, Figure 4. The extraction currents found from  $R_p$  are in good agreement with those derived from the Tafel plots and follow the same tip–substrate distance dependence, Figure 5. The latter also shows that the extraction currents are comparable in magnitude with the limiting currents for the ORR at all tip–substrate distances. These results therefore strongly suggest that the kinetics of the hydride oxidation is controlled by the diffusion of oxygen to the PdH tip. In the next section, we derive a simple mixed potential model to quantify the potential shift observed for different tip–substrate distances.

**The Mixed Potential Model.** One could argue that the potential shift observed in presence of oxygen reflects a pH change due to the ORR; if this were the case, the potential shift should be negative because the ORR makes the solution near the electrode more alkaline; experimentally the shift is always

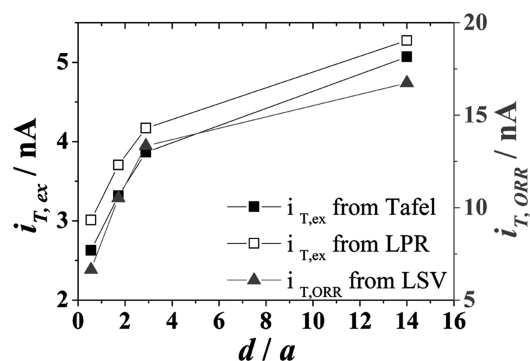


**Figure 5.** Comparison between the hydrogen extraction currents (left Y-axis) and the limiting currents for oxygen reduction (right Y-axis) recorded at different tip-substrate distances. The extraction currents were estimated from the Tafel plots and from the linear polarization resistances.

found to be positive. Instead the potentiometric and amperometric results suggest that the potential of the PdH tip obtained in the presence of dissolved oxygen is not the thermodynamic potential predicted from the phase rule but a mixed potential defined where the rate of anodic and cathodic processes are equal. This is akin to the mixed potential concept used in corrosion<sup>14</sup> and catalysis.<sup>15,16</sup> The main anodic reaction is the extraction of hydrogen from the hydride, while the main cathodic reaction is the ORR on the nanostructured Pd surface. The oxidation of the PdH can thus be thought of as a corrosion process. The larger the flux of oxygen, the higher the anodic current must be to match the reduction current. As a result, the tip potential shifts to more positive values as schematically shown in Figure 6 for three tip-substrate distances. When  $d =$

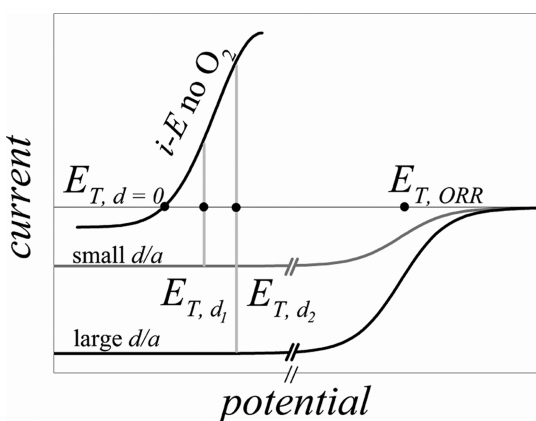


**Figure 6.** Schematic representation of the interplay between the current potential curves for the anodic (H extraction from PdH) and cathodic (ORR on the Pd surface) processes leading to a mixed potential different from the thermodynamic potential found in the absence of dissolved oxygen. To illustrate the dependence of the tip potential on the flux of oxygen, the sketch is drawn for three tip-substrate distances,  $d = 0 < d_1 < d_2$ .  $E_{T,ORR}$  is the half-wave potential for the ORR on the tip.

0, the diffusion of oxygen is fully hindered and  $E_{T,d=0}$  equals  $OCP_{\beta \rightarrow \alpha, no O_2}$ . At a distance  $d_1 > 0$ , hindrance has decreased and a small flux of oxygen forces the tip to take the mixed potential  $E_{T,d_1} > E_{T,d=0}$ . At the distance  $d_2 > d_1$ , hindrance is much less pronounced and a large flux of oxygen forces the tip to take the mixed potential  $E_{T,d_2}$  such that  $E_{T,d=0} < E_{T,d_1} < E_{T,d_2}$ . The

schematics also suggest that for any tip-substrate distance  $d$ , the mixed potential  $E_{T,d}$  can be simply estimated as a linear function of the diffusion-controlled current for the ORR at  $d$ ,  $i_{T,d,ORR}$ , via the polarization resistance recorded in the absence of oxygen,  $R_{p,no O_2}$ , the latter being the inverse of the current-potential curve of the PdH tip recorded in the absence of oxygen.

$$E_{T,d} = OCP_{\beta \rightarrow \alpha, no O_2} + |i_{T,d,ORR}| \times R_{p,no O_2} \quad (1)$$

This expression was tested for a nanostructured PdH microdisc with a small tip ( $a = 7.9 \mu m$ ,  $RG = \infty$ ) to enhance the flux of oxygen to the electrode and produce a larger potential shift. In this experiment, performed in a pH 7.5 phosphate buffer, all the parameters in the right-hand side of eq 1 were measured in the bulk so that the rate of ORR was at its maximum. Using the measured values for  $OCP_{\beta \rightarrow \alpha, no O_2}$  ( $-1000 \pm 3$  mV) and  $R_{p,no O_2}$  ( $21.6 M\Omega$ ), both recorded in Ar-purged solution, and of,  $i_{T,d,ORR}$  ( $-7.41$  nA) recorded in aerated solution, the calculated tip potential ( $-840$  mV) was in good agreement with the tip potential measured in the aerated pH 7.5 buffered solution ( $-844 \pm 3$  mV). Using the tip employed in Figure 2 ( $a = 18.7 \mu m$ ,  $RG = 3.3$ ), eq 1 was then tested against all tip-substrate distances by plotting the potentiometric approach curve ( $OCP_{\beta \rightarrow \alpha}$  vs  $d$ ) against the amperometric approach curve ( $i_{T,ORR}$  vs  $d$ ), both taken from Figure 2. Figure 7 shows a clear one to one correlation between the two

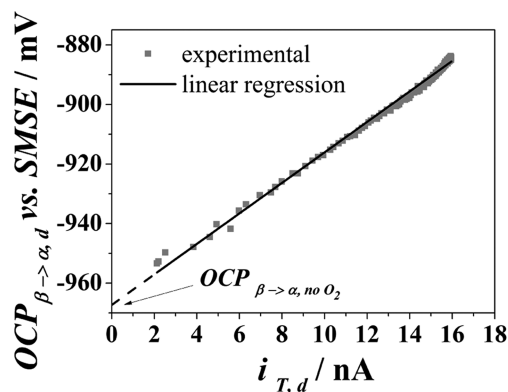


**Figure 7.** Plot of the tip potential recorded at different tip-substrate distances against the diffusion-controlled current for ORR recorded at the same tip-substrate distances. All experimental details as for Figure 2.

approach curves. Furthermore, the intercept ( $-967$  mV) which corresponds to a tip current equal to zero, as would be found with complete hindrance, is in perfect agreement with the thermodynamic potential measured in the absence of oxygen ( $OCP_{\beta \rightarrow \alpha, no O_2} = -973$  mV) in the pH 7 buffered solution; their difference is within the experimental error of 6 mV. The slope ( $4.48 M\Omega$ ) is in the same order of magnitude as  $R_{p,no O_2}$  obtained for this tip ( $26.8 M\Omega$ ). Despite the good agreement found in the bulk, eq 1 should only be valid for low oxygen fluxes where the potential shift remains sufficiently small that the PdH current-potential relationship is linear. For high oxygen fluxes, i.e., small tips in the bulk with large oxygen concentrations, the potential shift becomes so large that the PdH current-potential relationship becomes curved and the mixed potential is no longer a simple linear function of the limiting current for the ORR. This can be clearly seen on the



current potential curve recorded in the absence of oxygen with the small tip, Figure SI-5, Supporting Information. With small PdH nanostructured tips the high oxygen flux discharges hydrogen rapidly and the lifetime of the  $\beta$  to  $\alpha$  transition plateau becomes unworkably short. In oxygen-saturated solutions, it is difficult to observe a stable plateau with the 25  $\mu\text{m}$  diameter tips prepared as described above. With larger tips it is possible to deposit thicker nanostructured Pd films, thereby increasing the hydrogen reservoir, and operate in oxygen-saturated solutions. In conclusion, while eq 1 is qualitatively convenient to explain the correlation between potentiometric and amperometric approach curves, its quantitative use is limited to conditions such that the potential shift is no greater than ca. 50 mV; see in Supporting Information: Equation 1: Theoretical Approach and Validity.

To verify that the potentiometric response observed with the SECM tip was generic, similar experiments were conducted with a nanostructured Pd film deposited on a rotating disc electrode and loaded with hydrogen to  $\text{H}/\text{Pd} = 0.6$ . The potential of the electrode, recorded for several rotation rates in the aerated pH 7 phosphate buffer solution, was found to increase linearly with the square root of the rotation rate, Figure SI-6 (Supporting Information), and the intercept to be within 3 mV of the potential measured in Ar-purged solution. The RDE data therefore confirm the observations made with the SECM tip.

**Other Processes.** Such a mixed potential is not specific to the PdH system considered, and the methodology described here could therefore be extended to study localized and other forms of corrosion. For this, the tip would need to consist of the material of interest and the potentiometric response would be monitored for a range of tip–substrate distances above an inert substrate in the presence and absence of oxygen. For instance, the corrosion of a given alloy could be studied by fabricating a SECM tip from the alloy and recording its potentiometric response while approaching an inert surface in aerated solution. Alternatively, the substrate could be made from the sample of interest and the tip from an inert material. For example, the corrosion of a coated metallic surface could be investigated by approaching a submillimeter size polished glass disc toward a micrometre size pinhole, purposely made in the coating to behave as a microdisc.

Interestingly, replacing oxygen with a conventional redox mediator and operating with a large conducting substrate should enable the regeneration of the mediator at the substrate and enhance the rate of corrosion, thereby producing an increasingly positive potentiometric shift as the tip approaches the surface. The potentiometric approach curve would in this case follow the theory for positive feedback diffusion. This experiment was not tested with the PdH system because it dramatically shortens the lifetime of the  $\beta \rightarrow \alpha$  phase transition and it becomes impossible to measure a complete approach curve before the Pd nanostructure runs out of H.

The mixed potential should only affect potentiometric sensors capable of promoting a Faradaic process on their surface and is therefore not expected with potentiometric sensors where the electrode is separated from the analyte via a membrane, glass wall, or ionophore.

## CONCLUSION

The observations reported here clearly demonstrate that the potentiometric mode of SECM can be more complicated than anticipated; several remarks can now be made regarding this

mode: the tip is not necessarily a passive probe as normally assumed, and one should consider the possibility of redox processes occurring on its surface even when held at zero current. Redox processes may force the tip potential to differ from the expected thermodynamic value by taking a mixed potential if the tip surface is able to promote two Faradaic processes with equal and opposite rates. Furthermore, the potentiometric response can be controlled by diffusion provided one of the species involved in the Faradaic processes reacts with the tip at a diffusion-controlled rate. Under these conditions, the potentiometric approach curve becomes diffusion-controlled and akin to the traditional SECM approach curves found in the amperometric feedback mode. Overall, the tip potential becomes sensitive to the tip–substrate distance and less so to the activity of a target species, as initially intended. These effects must be added to the dependence of the tip potential on Ohmic drop when current flows between other electrodes in the cell. One should not see the above as restrictions; the ability to finely control the mixed potential by simple adjustment of the tip–substrate distance opens new opportunities for the potentiometric mode of SECM. Regarding the PdH system, our results clearly show that the presence of an oxidant capable of extracting H will significantly affect the pH measurement. The strong tip–substrate dependence makes use of such an electrode in SECM very challenging, as it becomes difficult to relate variations in tip potential to pH. This is particularly relevant when the flux of oxidant toward the tip is high as for example found with small tips or with a substrate capable of regenerating the mediator.

## ASSOCIATED CONTENT

### Supporting Information

Additional material as described in the text. This material is available free of charge via the Internet at <http://pubs.acs.org>.

## AUTHOR INFORMATION

### Corresponding Author

\*E-mail: [gd@soton.ac.uk](mailto:gd@soton.ac.uk)

### Notes

The authors declare no competing financial interest.

## ACKNOWLEDGMENTS

This work was funded by EPSRC grants EP/I001204 and EP/I001956. G.D. also thanks the HanseWissenschaftskolleg, Institute for Advanced Study, Delmenhorst, Germany, for the award of a fellowship.

## REFERENCES

- (1) Denuault, G.; Nagy, G.; Toth, K. In *Scanning Electrochemical Microscopy*, 2nd ed.; Bard, A. J., Mirkin, M. V., Eds.; CRC Press: Boca Raton, FL, 2012; p 275.
- (2) Denuault, G.; Frank, M. H. T.; Peter, L. M. *Faraday Discuss.* **1992**, 23.
- (3) Lewis, F. *The Palladium Hydrogen System*; Academic Press: London, 1976.
- (4) Vasile, M. J.; Enke, C. G. *J. Electrochem. Soc.* **1965**, 112, 865.
- (5) Wolfe, R. C.; Weil, K. G.; Shaw, B. A.; Pickering, H. W. *J. Electrochem. Soc.* **2005**, 152, B82.
- (6) Imokawa, T.; Williams, K.-J.; Denuault, G. *Anal. Chem.* **2006**, 78, 265.
- (7) Attard, G. S.; Bartlett, P. N.; Coleman, N. R. B.; Elliott, J. M.; Owen, J. R.; Wang, J. H. *Science* **1997**, 278, 838.
- (8) Guerin, S.; Attard, G. S. *Electrochem. Commun.* **2001**, 3, 544.
- (9) Serrapede, M.; Denuault, G. *In preparation*.

- (10) Cornut, R.; Lefrou, C. *J. Electroanal. Chem.* **2007**, 608, 59.
- (11) Burke, L. D.; Casey, J. K. *J. Electrochem. Soc.* **1993**, 140, 1284.
- (12) Burke, L. D.; Casey, J. K. *J. Appl. Electrochem.* **1993**, 23, 573.
- (13) Birkin, P. R.; Elliott, J. M.; Watson, Y. E. *Chem. Commun.* **2000**, 1693.
- (14) Power, G. P.; Ritchie, I. M. *Electrochim. Acta* **1981**, 26, 1073.
- (15) Park, J. H.; Zhou, H.; Percival, S. J.; Zhang, B.; Fan, F.-R. F.; Bard, A. J. *Anal. Chem.* **2013**, 85 (2), 964–970.
- (16) Selzer, Y.; Turyan, I.; Mandler, D. *J. Phys. Chem. B* **1999**, 103, 1509.